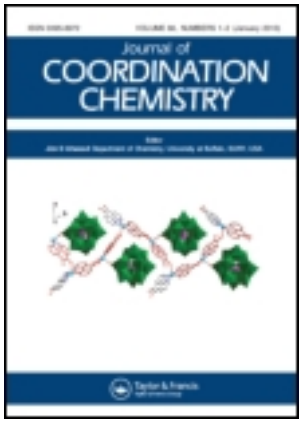

Journal of Coordination Chemistry
Publication details, including instructions for authors and subscription information:
http://www.tandfonline.com/loi/gcoo20

DNA-binding, antioxidant activity, and bioactivity studies of ruthenium(II) complexes containing amino substituents

Yang-Yin Xie [a], Guang-Bin Jiang [a], Jun-Hua Yao [b], Gan-Jian Lin [a], Hong-Liang Huang [c], Xiu-Zhen Wang [a] & Yun-Jun Liu [a]

[a] School of Pharmacy, Guangdong Pharmaceutical University, Guangzhou, P.R. China

[b] Instrument Analysis and Research Center, Sun Yat-Sen University, Guangzhou, P.R. China

[c] School of Life Science and Biopharmaceutical, Guangdong Pharmaceutical University, Guangzhou, P.R. China

Published online: 20 Jun 2013.

To cite this article: Yang-Yin Xie, Guang-Bin Jiang, Jun-Hua Yao, Gan-Jian Lin, Hong-Liang Huang, Xiu-Zhen Wang & Yun-Jun Liu (2013) DNA-binding, antioxidant activity, and bioactivity studies of ruthenium(II) complexes containing amino substituents, Journal of Coordination Chemistry, 66:14, 2423-2433, DOI: 10.1080/00958972.2013.805214

To link to this article: http://dx.doi.org/10.1080/00958972.2013.805214

Journal of Coordination Chemistry, 2013
Vol. 66, No. 14, 2423–2433, http://dx.doi.org/10.1080/00958972.2013.805214

DNA-binding, antioxidant activity, and bioactivity studies of ruthenium(II) complexes containing amino substituents

YANG-YIN XIE†, GUANG-BIN JIANG†, JUN-HUA YAO‡, GAN-JIAN LIN†, HONG-LIANG HUANG*§, XIU-ZHEN WANG† and YUN-JUN LIU*†

†School of Pharmacy, Guangdong Pharmaceutical University, Guangzhou, P.R. China
‡Instrument Analysis and Research Center, Sun Yat-Sen University, Guangzhou, P.R. China
§School of Life Science and Biopharmaceutical, Guangdong Pharmaceutical University, Guangzhou, P.R. China

(*Received 24 January 2013; in final form 25 March 2013*)

Two new Ru(II) complexes, $[Ru(dmp)_2(dadppz)](ClO_4)_2$ (**1**) and $[Ru(dip)_2(dadppz)](ClO_4)_2$ (**2**), were synthesized and characterized by elemental analysis, ES-MS, and ^1H NMR. DNA-binding behaviors were investigated by absorption titration and luminescence spectra. The DNA-binding constants were 3.1 ($\pm$ 0.2) $\times 10^4$ and 3.0 ($\pm$ 0.2) $\times 10^5\,M^{-1}$ for **1** and **2**. The antioxidant activity of these complexes against hydroxyl radical (·OH) was explored. The cytotoxicities *in vitro* towards A549, BEL-7402, MG-63, and SKBR-3 cells were studied by 3-(4,5dimethylthiazol-2-yl)-2,5-diphenyltetrazolium bromide method. Complex **1** shows high cytotoxicity, but **2** is not cytotoxic towards the selected cell lines. Apoptosis and cell cycle distribution were studied by flow cytometry. The cellular uptake showed that complexes can enter into the cytoplasm. JC-1 was used as a fluorescence probe in detecting the mitochondrial membrane potential and results indicate that the mitochondrial membrane potential decreases.

Keywords: Ruthenium(II) complexes; DNA-binding; Antioxidant activity; Bioactivity

1. Introduction

Binding of small molecules with DNA has been studied extensively. Small molecules possessing DNA-binding abilities include metal complexes, porphyrins, natural antibiotics, simple aromatic hydrocarbons, and some heterocyclic cations [1–6]. Among metal complexes, the binding of ruthenium complexes to DNA has been paid great attention [7–14]. $[Ru(phen)_2(mitatp)]^{2+}$ (mitatp = 5-methoxy-isatino[1,2-b]-1,4,8,9-tetraazatriphenylene) binds to DNA with a large affinity ($2.77 \times 10^6\,M^{-1}$) [15]. $[Ru(phen)_2(bfipH)]^{2+}$ (bfipH = 2-(benzofuran-2yl)imidazo[4,5-f][1,10]phenanthroline) is an efficient dual inhibitor of topoisomerases I and II [16]. $[Ru(bpy)_2(dppz)]^{2+}$ (dppz = dipyrido[3,2-*a*:2′,3′-*c*]phenazine) shows no luminescence in aqueous solution, but luminesces brightly upon binding to DNA, displaying the characteristic of a "molecular light switch" [17–21]. Ruthenium complexes

*Corresponding authors. Email: hhongliang@163.com (H.L. Huang); lyjche@163.com (Y.J. Liu)

also exhibit significant antitumor activity; $[Ru(dmb)_2(BHIP)]^{2+}$ (BHIP = 2-(3-bromo-4-hydroxyphenyl)imizado[4,5-f][1,10]phenanthroline) can suppress the growth of HeLa cells with a low IC_{50} value [22]. $[Ru(bpy)_2(dppz)]^{2+}$ effectively inhibits the proliferation of HT-29 cells [23]. Since complexes containing dppz show large DNA-binding affinity and significant antitumor activity, in this article we synthesize a derivative of dppz and two Ru(II) complexes $[Ru(dmp)_2(dadppz)]^{2+}$ (dadppz = 11,12-diaminodipyrido[3,2-*a*:2′,3′-*c*]phenazine, dmp = 2,9-dimethyl-1,10-phenanthroline) (**1**) and $[Ru(dip)_2(dadppz)]^{2+}$ (di*p* = 4,7-diphenyl-1,10-phenanthroline, scheme 1) (**2**). In order to observe the DNA-binding and cytotoxic activity of the two complexes, DNA-binding behaviors were studied by absorption titration and luminescence spectra. The cytotoxicities *in vitro* of **1** and **2** were investigated by 3-(4,5dimethylthiazol-2-yl)-2,5-diphenyltetrazolium bromide (MTT) method. The apoptosis and cell cycle arrest on BEL-7402 cells were performed by flow cytometry. The cellular uptake and mitochondrial membrane potential were studied by fluorescence microscopy. The antioxidant activity against hydroxyl radicals (·OH) was also explored.

2. Experimental

2.1. *Materials and methods*

All reagents and solvents were purchased commerially and used without purification unless noted; Ultrapure MilliQ water was used in all experiments. Dimethyl sulfoxide (DMSO), 2,9-dimethyl-1,10-phenanthroline (dmp), 4,7-diphenyl-1,10-phenanthroline (dip), and RPMI 1640 were purchased from Sigma. Cell lines of A549, BEL-7402, MG-63, and SKBR-3 were purchased from American Type Culture Collection. $RuCl_3 \cdot xH_2O$ was purchased from Kunming Institute of Precious Metals. 1,10-Phenanthroline was obtained from Guangzhou Chemical Reagent Factory.

Microanalysis (C, H, and N) was carried out with a Perkin-Elmer 240Q elemental analyzer. Electrospray ionization mass spectra (ES-MS) were recorded on a LCQ system (Finnigan MAT, USA) using methanol as mobile phase. The spray voltage, tube lens offset, capillary voltage, and capillary temperature were set at 4.50 kV, 30.00 V, 23.00 V, and 200 °C, respectively, and the quoted *m/z* values are for the major peaks in the isotope

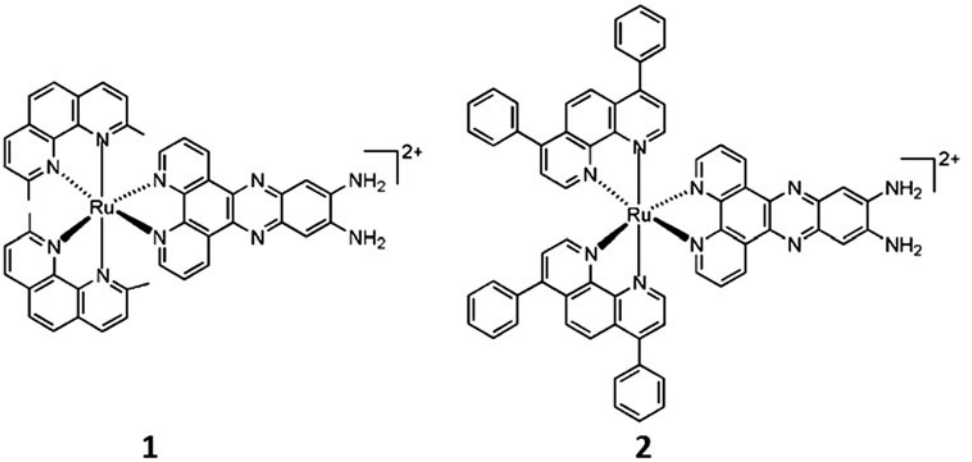

1 **2**

Scheme 1. The structures of **1** and **2**.

distribution. ^{1}H NMR and ^{13}C NMR spectra were recorded on a Varian-500 spectrometer with DMSO [D_6] as solvent and tetramethylsilane as an internal standard at 500 MHz at room temperature.

2.2. *Synthesis of ligand dadppz and complexes*

2.2.1. Synthesis of ligand dadppz. dadppz was synthesized according to modified method [24]. Briefly, a mixture of 1,10-phenanthroline-5,6-dione (0.252 g, 1.2 mM), 1,2,4,5-benzenetetramine tetrahydrochloride (0.341 g, 1.2 mM), and potassium carbonate (0.331 g, 2.4 mM) in ethanol (50 mL) and H_2O (5 mL) was refluxed under argon for 40 min. After the reaction mixture was allowed to stand at room temperature, the precipitate was filtered and washed with 10 mL ethanol. The filtrate was evaporated under reduced pressure to 5 mL. Upon cooling, a red precipitate was obtained by dropwise addition of water. ES-MS (CH_3CN, *m/z*): 313.3 $[M+1]^+$.

2.2.2. Synthesis of $[Ru(dmp)_2(dadppz)](ClO_4)_2$ (1). A mixture of *cis*-$[Ru(dmp)_2Cl_2]\cdot 2H_2O$ [25] (0.312 g, 0.5 mmol) and dadppz (0.156 g, 0.5 mmol) in ethanol (70 cm^3) was refluxed under argon for 2 h to give a clear red solution and the solvent was removed to 10 cm^3 under reduced pressure. Upon cooling, a red precipitate was obtained by dropwise addition of saturated aqueous $NaClO_4$ solution. The crude product was purified by column chromatography on neutral alumina with a mixture of CH_3CN–C_2H_5OH (4 : 1, v/v) as eluent. The red band was collected. The solvent was removed under reduced pressure and a red powder was obtained. Yield: 69%. Anal. Calcd for $C_{46}H_{36}N_{10}Cl_2O_8Ru$: C, 53.70; H, 3.53; N, 13.61%. Found: C, 53.52; H, 3.38; N, 13.78%. ^{1}H NMR (DMSO-d_6, ppm): δ 9.28 (d, 2H, J = 7.0 Hz), 8.91 (d, 2H, J = 8.0 Hz), 8.43 (dd, 4H, J = 8.5, J = 8.5 Hz), 8.25 (d, 2H, J = 8.5 Hz), 7.98 (d, 2H, J = 8.0 Hz), 7.49 (dd, 4H, J = 5.5, J = 5.5 Hz), 7.40–7.35 (m, 2H), 7.11 (s, 2H), 6.29 (s, 4H), 2.92 (s, 6H), 2.50 (s, 6H). ES-MS (CH_3CN): *m/z* 928.9 ($[M\text{-}ClO_4]^+$), 829.2 ($[M\text{-}2ClO_4\text{-}H]^+$), 415.3 ($[M\text{-}2ClO_4]^{2+}$).

2.2.3. Synthesis of $[Ru(dip)(dadppz)](ClO_4)_2$ (2). This complex was synthesized according to the modified procedure and in a manner identical to that described for **1**, with *cis*-$[Ru(dip)_2Cl_2]\cdot 2H_2O$ [26] in place of *cis*-$[Ru(dmp)_2Cl_2]\cdot 2H_2O$. Yield: 70%. Anal. Calcd for $C_{66}H_{44}N_{10}Cl_2O_8Ru$: C, 62.07; H, 3.47; N, 10.97%. Found: C, 62.36; H, 3.60; N, 10.82%. ^{1}H NMR (DMSO-d_6, ppm): δ 9.53 (d, 2H, J = 8.0 Hz), 8.35 (dd, 4H, J = 5.5, J = 5.0 Hz), 8.28 (s, 4H), 8.20 (d, 2H, J = 5.5 Hz), 7.92–7.89 (m, 2H), 7.82 (d, 2H, J = 5.5 Hz), 7.78 (d, 2H, J = 5.5 Hz), 7.71–7.60 (m, 20H), 7.21 (s, 2H), 6.61 (s, 4H). ES-MS (CH_3CN): *m/z* 1177.1 ($[M\text{-}ClO_4]^+$), 539.5 ($[M\text{-}2ClO_4]^{2+}$).

Caution: Perchlorate salts of metal compounds with organic ligands are potentially explosive, and only small amounts of the material should be prepared and handled with great care.

2.3. *DNA-binding studies*

The DNA-binding experiments were performed at room temperature. Buffer (5 mM Tris, 50 mM NaCl, pH 7.0) was used for absorption titration and luminescence titration. The absorption titration of Ru(II) complexes with increasing DNA in buffer were performed on a Shimadzu UV-3101PC spectrophotometer at room temperature.

Titrations of the complex in buffer were performed using a fixed concentration (20 μM) for complex to which increments of the DNA stock solution were added. Ru-DNA solutions were allowed to incubate for 5 min before the absorption spectra were recorded. The intrinsic binding constants K, based on the absorption titration, were measured by monitoring changes of absorption in the MLCT band with increasing concentration of DNA using the following equation [27],

$$[\mathrm{DNA}]/(\varepsilon_a - \varepsilon_f) = [\mathrm{DNA}]/(\varepsilon_b - \varepsilon_f) + 1/[K_b((\varepsilon_b - \varepsilon_f)]$$

where [DNA] is the concentration of DNA in base pairs, ε_a, ε_f and ε_b correspond to the apparent absorption coefficient Aobsd/[Ru], the extinction coefficient for the free ruthenium complex and the extinction coefficient for the ruthenium complex in the fully bound form, respectively. In plots of $[\mathrm{DNA}]/(\varepsilon_a - \varepsilon_f)$ *versus* [DNA], K_b is given by the ratio of slope to intercept.

2.4. *Scavenger measurements of hydroxyl radical (*·OH)

The hydroxyl radical (·OH) in aqueous media was generated by the Fenton system [28]. The solution of the tested complexes was prepared with DMF. The 5 ml of assay mixture contained the following reagents: safranin (28.5 μM), EDTA-Fe(II) (100 μM), H_2O_2 (44.0 μM), the tested compounds (0.25–1.75 μM), and a phosphate buffer (67 mM, pH = 7.4). The assay mixtures were incubated at 37 °C for 30 min in a water bath, after which the absorbance was measured at 520 nm. All the tests were run in triplicate and expressed as the mean. A_i was the absorbance in the presence of the tested compound; A_0 was the absorbance in the absence of tested compounds; A_c was the absorbance in the absence of tested compound, EDTA-Fe(II), H_2O_2. The suppression ratio (η_a) was calculated on the basis of $(A_i - A_0)/(A_c - A_0) \times 100\%$.

2.5. *Cytotoxicity assay in vitro*

MTT assay procedures were used [29]. Cells were placed in 96-well microassay culture plates (8×10^3 cells per well) and grown overnight at 37 °C in a 5% CO_2 incubator. Complexes tested were then added to the wells to achieve final concentrations ranging from 10^{-6} to 10^{-4} M. Control wells were prepared by addition of culture medium (100 μL). The plates were incubated at 37 °C in a 5% CO_2 incubator for 48 h. Upon completion of the incubation, stock MTT dye solution (20 μL, 5 mg mL^{-1}) was added to each well. After 4 h, buffer (100 μL) containing DMF (50%) and sodium dodecyl sulfate (20%) was added to solubilize the MTT formazan. The optical density of each well was then measured with a microplate spectrophotometer at 490 nm. The IC_{50} values were determined by plotting the percentage viability *versus* concentration on a logarithmic graph and reading off the concentration at which 50% of cells remain viable relative to the control. Each experiment was repeated at least thrice to obtain the mean values. Four different tumor cell lines were studied: A549 (Human lung adenocarcinoma cell Line), BEL-7402 (Human hepatocellular carcinoma cell line), MG-63 (Human osteosarcoma cell line), and SKBR-3 (Human breast cancer cell line).

2.6. *Apoptosis assay by flow cytometry*

After chemical treatment, 1×10^6 cells were harvested, washed with PBS, then fixed with 70% ethanol, and finally, maintained at 4 °C for at least 24 h. Then, the pellets were stained with the fluorescent probe solution containing 50 μg mL^{-1} PI and 1 mg mL^{-1} annexin in PBS on ice in the dark for 15 min. Then the fluorescence emission was measured at 530 and 575 nm (or equivalent) using 488 nm excitation by a FACS Calibur flow cytometer (Beckman Dickinson & Co., Franklin Lakes, NJ). A minimum of 10,000 cells were analyzed.

2.7. *Cellular uptake*

BEL-7402 cells were placed in 24-well microassay culture plates (4×10^4 cells per well) and grown overnight at 37 °C in a 5% CO_2 incubator. Complex **2** was then added to the wells. The plates were incubated at 37 °C in a 5% CO_2 incubator for 24 h. Upon completion of the incubation, the wells were washed thrice with phosphate buffered saline (PBS); after discarding the culture medium, the cells were visualized by fluorescence microscopy.

2.8. *Cell cycle arrest by cytometric analysis*

BEL-7402 and SKBR-3 cells were seeded into six-well plates (Costar, Corning Corp, New York) at a density of 2×10^5 cells per well and incubated for 24 h. The cells were cultured in RPMI 1640 supplemented with fetal bovine serum (10%) and incubated at 37 °C and 5% CO_2. The medium was removed and replaced with medium (final DMSO concentration, 1% v/v) containing 1 (black) (50 μM). After incubation for 24 h, the cell layer was trypsinized and washed with cold PBS and fixed with 70% ethanol. 20 μL of RNAse (0.2 mg mL^{-1}) and 20 μL of propidium iodide (PI) (0.02 mg mL^{-1}) were added to the cell suspensions and incubated at 37 °C for 30 min. Then, the samples were analyzed with a FACSCalibur flow cytometer (Becton Dickinson & Co., Franklin Lakes, NJ). The number of cells analyzed for each sample was 10,000 [30].

2.9. *Mitochondrial membrane potential assay*

Cells were treated for 24 h with complex in 12-well plates and then washed thrice with cold PBS. The cells were then detached with trypsin-EDTA solution. Collected cells were incubated for 20 min with 1 μg mL^{-1} of JC-1 (5,5′,6,6′-tetrachloro-1,1′,3,3′-tetraethylbenzimidazolcarbocyanine iodide) in culture medium at 37 °C in the dark. Cells were immediately centrifuged to remove the supernatant. Cell pellets were suspended in PBS and then imaged under microscope.

3. Results and discussion

3.1. *Synthesis and characterization*

The ligand dadppz was prepared through condensation of 1,10-phenanthroline-5,6-dione with 1,2,4,5-benzenetetramine tetrahydrochloride using a method similar to that reported [24]. The corresponding ruthenium(II) mixed-ligand complexes were synthesized by direct reaction of dadppz with the appropriate precursor complexes in ethanol. The desired

ruthenium(II) complexes were isolated as the perchlorates and purified by column chromatography. In the ES-MS spectra for the Ru(II) complexes, all of the expected signals $[M\text{-}ClO_4]^+$, $[M\text{-}2ClO_4\text{-}H]^+$, and $[M\text{-}2ClO_4]^{2+}$ were observed (Supplementary material) The measured molecular weights were consistent with the expected values. In the IR spectra, 3369 cm^{-1} for **1** and 3364 cm^{-1} for **2** are characteristic of N–H stretch; 2925 cm^{-1} for **1** is the C–H stretch (Supplementary material). Two singlets at 6.29 ppm for **1** and 6.61 ppm for **2** are assigned to NH_2. These data show that **1** and **2** were synthesized.

3.2. *Electronic absorption titration*

The electronic absorption spectra of **1** and **2** in the absence and presence of CT-DNA are given in figure 1. As DNA concentration is increased, MLCT bands of **1** at 453 and **2** at 464 nm exhibit hypochromism of about 24.2 and 23.3%, and bathochromism of 5 and 3 nm, respectively. These spectral characteristics suggest a stacking interaction between the aromatic chromophore and the DNA base pairs.

To further elucidate the binding strength of the complexes, the intrinsic constants K_b are determined by monitoring the changes in absorbance of the MLCT band with increasing concentration of CT-DNA. The values of K_b are determined to be 3.1 ($\pm$ 0.2) $\times 10^4$ and 3.0 ($\pm$ 0.2) $\times 10^5$ M^{-1} for **1** and **2**, respectively. These values are smaller than those of $[Ru(bpy)_2(dppz)]^{2+}$ (4.9×10^6 M^{-1}, dppz = dipyrido[2,3-*a*:3′,2′-*c*]phenazine) [21] and $[Ru(bpy)_2(HBT)]^{2+}$ (5.71 ($\pm$ 0.20) $\times 10^7$ M^{-1}, HBT = 11*H*, 13*H*-4, 5, 9, 10, 12, 14-hexaazabenzo [*b*] triphenylene) [31], but comparable to that of $[Ru(dmp)_2(dcdppz)]^{2+}$ (1.78×10^5 M^{-1}, dcdppz = 7, 8-dichlorodipyrido[3,2-*a*:2′,3′-*c*]phenazine) [32].

3.3. *Luminescence spectroscopy*

At room temperature, **1** shows no luminescence and **2** exhibits luminescence in Tris buffer with a maximum at 594 nm. The luminescence spectra of **2** in the presence of CT-DNA in buffer solution are shown in figure 2. As the concentrations of DNA increased, the emission intensity of **2** was 4.02 times larger than the original, implying that **2** can interact with CT-DNA and be protected by DNA efficiently, since the hydrophobic environment inside

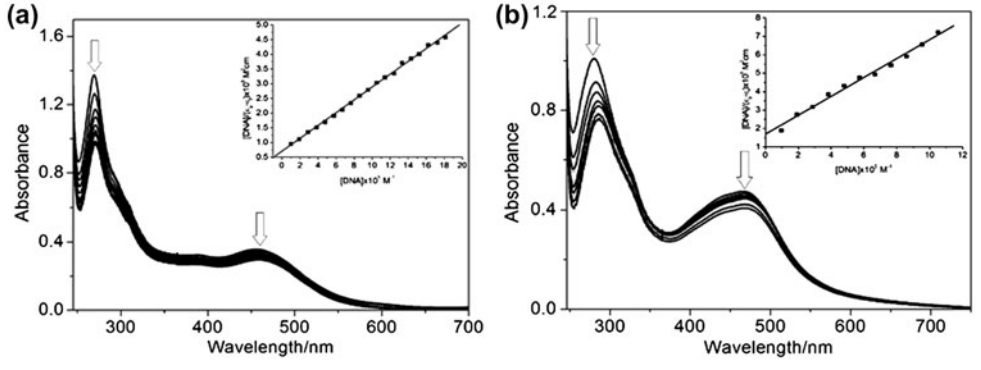

Figure 1. Absorption spectra of complexes in Tris-HCl buffer upon addition of CT DNA in the presence of (a) **1** and (b) **2**. [Ru] = 20 μM. Arrow shows the absorbance change upon increase of DNA concentration. Plots of $[DNA]/(\varepsilon_a - \varepsilon_f)$ *vs.* [DNA] for the titration of DNA with Ru(II) complexes.

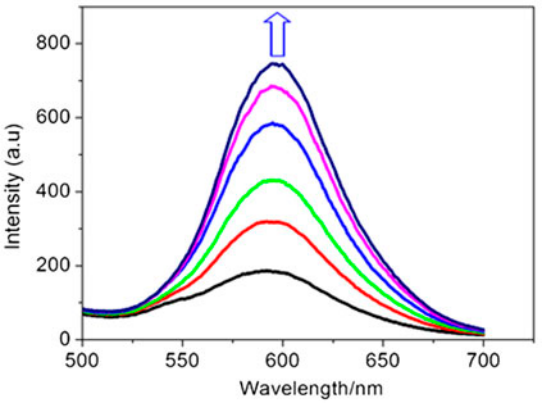

Figure 2. Emission spectra of **2** in Tris-HCl buffer in the absence and presence of CT-DNA. Arrow shows the intensity change upon increasing DNA concentrations.

Table 1. Scavenging ratio (%) of complexes against ·OH.

	Average inhibition (%) for ·OH						
Complex	0.25	0.50	0.75	1.0	1.25	1.50	1.75 (μM)
1	0.25	17.09	43.22	51.01	62.31	68.59	72.86
2	0.52	10.68	37.76	52.60	64.84	73.96	77.86

the DNA helix reduces the accessibility of water to the complex and the complex mobility is restricted at the binding site, leading to the decrease of vibrational modes of relaxation.

3.4. *Antioxidant activity against hydroxyl radical*

Hydroxyl radical (·OH) production can result in cell membrane protein damage. It has been reported that the free radical-scavenging ability of chromones is excellently directed toward hydroxyl radical [33]. The antioxidant activities on hydroxyl radicals of **1** and **2** were studied (table 1). As shown in figure 3, the suppress ratio against ·OH ranged from 0.25 to 72.86% for **1**, 0.52 to 77.86% for **2**. The inhibitory effect of **1** and **2** on ·OH was concentration related and the suppression ratio increased with increasing complex concentration of 0.25–1.75 μM. At low concentration, the antioxidant activity of **1** is higher than **2**, however, **2** shows higher antioxidant activity than **1** at high concentration. It may be believed that the information obtained from the present work would ultimately be helpful to develop new potential antioxidants and new therapeutic reagents for some diseases.

3.5. *Cytotoxicity assay in vitro*

The cytotoxicities *in vitro* of **1** and **2** on A549, BEL-7402, MG-63, and SKBR-3 cell lines were assayed by MTT method. After exposure to different concentrations of **1** and **2** for 48 h, the IC_{50} values were calculated and are listed in table 2. Unexpectedly, **2** shows no cytotoxicity toward the above tumor cell lines. Complex **1** exhibits high cytotoxic activities

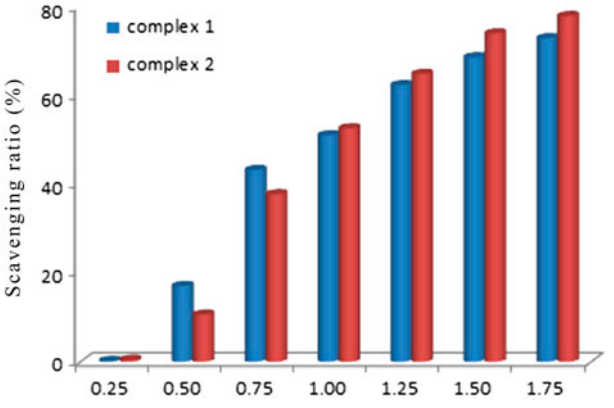

Figure 3. Scavenging effect of **1** and **2** on hydroxyl radicals. Experiments were performed in triplicate.

Table 2. The IC_{50} values of **1** and **2** against selected cell lines.

	IC_{50} (μM)			
Complex	A549	BEL-7402	MG-63	SKBR-3
1	25.7 ± 2.4	16.4 ± 1.5	11.0 ± 1.1	10.6 ± 1.4
2	>100	>100	>100	>100
Cisplatin	11.2 ± 1.3	7.4 ± 1.5	6.5 ± 0.7	–

against the selected tumor cell lines, more sensitive on MG-63 (IC_{50} = 11.0 μM) and SKBR-3 (IC_{50} = 10.6 μM) than toward A549 (IC_{50} = 25.7 μM) and BEL-7402 (IC_{50} = 16.4 μM) cells; its cytotoxicity is lower than cisplatin under identical conditions. Cell viability is concentration dependent (figure 4), with increasing concentrations of **1**, an obvious decrease is observed for cell viability. These results imply that **1** is cytotoxic against different tumor cell lines.

3.6. *Apoptosis assay by flow cytometry*

Apoptosis is the process of programed cell death that may occur in multicellular organisms. Biochemical events lead to characteristic cell changes (morphology) and death. In order to determine the percentage of apoptotic and necrotic cells, the apoptosis was performed with BEL-7402 cells exposure to different concentrations of **1** for 24 h. As shown in Supplementary material, in the control (a), the percentage of necrotic and apoptotic cells are 0.01 and 0.00%. Treatment of BEL-7402 with 25 (b) and 50 μM (c) **1**, the percentage of necrotic and apoptotic cells are 0.70 and 5.21, 4.41, and 13.51%, respectively. These results show that **1** can effectively induce BEL-7402 cell apoptosis, and the apoptotic effect is closely related to the concentrations of **1**.

3.7. *Cellular uptake studies*

The uptake of **2** by BEL-7402 cells was studied; 12.5 μM complex **2** was added to the wells (4×10^4 cells per well) and incubated at 37 °C in a 5% CO_2 incubator for 24 h.

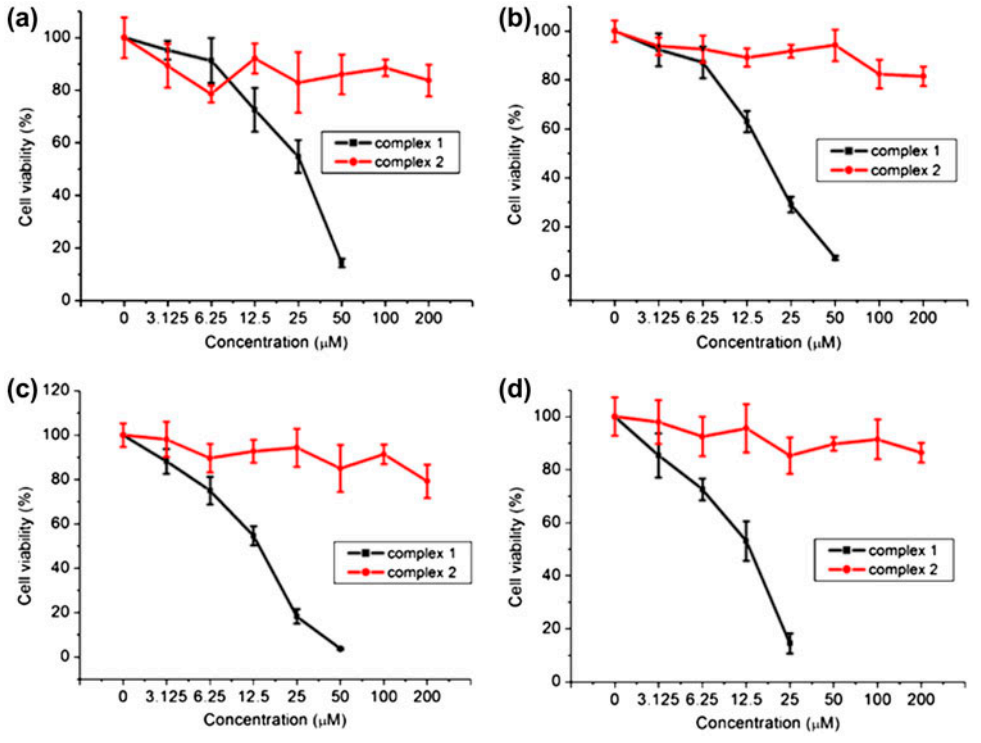

Figure 4. Cell viability of **1** and **2** on A549 (a) BEL-7402 (b) MG-63 (c) and SKBR-3 (d) cells proliferation *in vitro*. Each point is the mean ± standard error obtained from three independent experiments.

Then the cells were observed under fluorescence microscope (Supplementary material). In the presence of 12.5 μM of **2**, bright red fluorescent spots in the images were observed. The results show that **2** can be uptaken by cells and can enter into the cytoplasm and accumulate in the nuclei.

3.8. *Cell cycle arrest studies*

The effect of **1** on the cell cycle of BEL-7402 and SKBR-3 cells was studied by flow cytometry in PI-stained cells after the two cell lines were treated with 50 μM of **1** for 24 h. The representative DNA distribution histograms of BEL-7402 (a) and SKBR-3 (b) cells in the presence of **1** are shown in figure 5. With treatment of BEL-7402 cells, an obvious enhancement (6.60%) in the percentage of cells at S phase was observed, accompanied by a corresponding reduction in the percentage of cells in the G0/G1 and G2/M phases. These results indicate that the antiproliferative mechanism induced by **1** on BEL-7402 cells is S phase and on SKBR-3 cells is G2/M phase arrest. We also conclude that the same complex displays different antitumor mechanism toward different tumor cell lines.

3.9. *Mitochondrial membrane potential detection*

JC-1 was used as a fluorescence probe in assaying the change of mitochondrial membrane potential. JC-1 forms aggregates and emits a red fluorescence at high mitochondrial

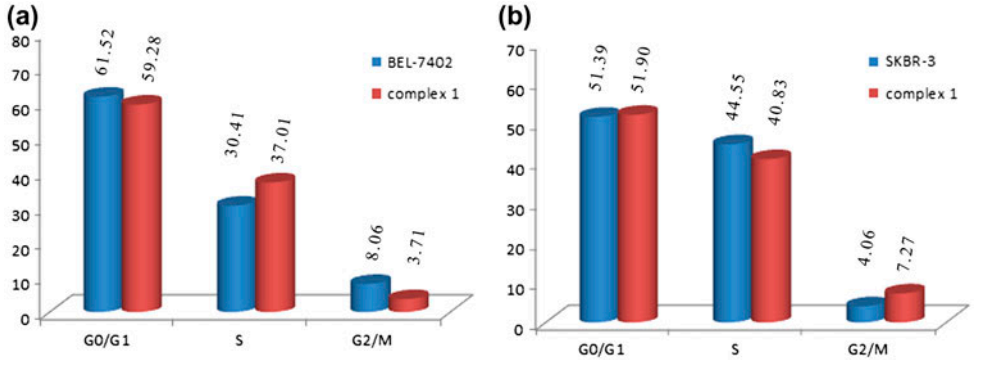

Figure 5. Cell cycle distribution of BEL-7402 (a) and SKBR-3 (b) cells exposed to 50 μM **1** for 24 h.

membrane potential. When the values of the mitochondrial membrane potential are low, JC-1 forms monomers, which emit green fluorescence. After BEL-7402 cells are exposed to 12.5 μM **1** for 24 h, the change of mitochondrial membrane potential is shown in Supplementary material. In the control (a), JC-1 exhibits red fluorescence (JC-1 aggregates) accompanied by high mitochondrial membrane potential. In the presence of **1** (b), JC-1 emits green fluorescence (JC-1 monomers) corresponding to low mitochondrial membrane potential. The change in fluorescence from red to green indicates decrease of mitochondrial membrane potential. These results suggest that **1** induces apoptosis in BEL-7402 cells through the mitochondrial signal transduction pathway.

4. Conclusions

Two new Ru(II) complexes, $[Ru(dmp)_2(dadppz)]^{2+}$ (**1**) and $[Ru(dip)_2(dadppz)]^{2+}$ (**2**), were synthesized and characterized. The DNA-binding shows that **1** and **2** bind to CT-DNA. Complex **1** demonstrates high cytotoxic activity against the selected tumor cell lines, while **2** shows little cytotoxicity towards these cell lines under the same experimental conditions. The cytotoxic activity is not consistent with the DNA-binding strength. Complex **1** can effectively induce apoptosis in BEL-7402 cells. The cell cycle assay exhibits that the antiproliferative mechanism induced by **1** on BEL-7402 cells is S phase and on SKBR-3 cells is G2/M phase arrest. Mitochondrial membrane potential detection shows that **1** induces apoptosis in BEL-7402 cells through the mitochondrial signal transduction pathway.

Acknowledgments

This work was financially supported by the National Nature Science Foundation of China (No. 31070858) and Guangdong Pharmaceutical University.

References

[1] Y. An, Y.Y. Lin, H. Wang, H.Z. Sun, M.L. Tong, L.N. Ji, Z.W. Mao. *Dalton Trans.*, **12**, 1250 (2007).
[2] C.M. Che, M. Yang, K.H. Wong, H.L. Chan, W. Lam. *Chem. Eur. J.*, **5**, 3350 (1999).
[3] B. Chen, S. Wu, A. Li, F. Liang, X. Zhou, X. Cao, Z. He. *Tetrahedron*, **62**, 5487 (2006).

[4] C.Y. Wei, G.Q. Jia, J.L. Yuan, Z.C. Feng, C. Li. *Biochemistry*, **45**, 6681 (2006).
[5] A.A. Ghazaryan, Y.B. Dalyan, S.G. Haroutiunian, A. Tikhomirova, N. Taulier, J.W. Wells, T.V. Chalikian. *J. Am. Chem. Soc.*, **128**, 1914 (2006).
[6] V. Uma, M. Elango, B.U. Nair. *Eur. J. Inorg. Chem.*, **22**, 3484 (2007).
[7] S. Shi, X.T. Geng, J. Zhao, T.M. Yao, C.R. Wang, D.J. Yang, L.F. Zheng, L.N. Ji. *Biochimie*, **92**, 370 (2010).
[8] Z.H. Liang, Z.Z. Li, H.L. Huang, Y.J. Liu. *J. Coord. Chem.*, **64**, 3342 (2011).
[9] H.L. Huang, Z.Z. Li, X.Z. Wang, Z.H. Liang, Y.J. Liu. *J. Coord. Chem.*, **65**, 3287 (2012).
[10] L.F. Tan, J.L. Shen, X.J. Chen, X.L. Liang. *DNA Cell Biol.*, **28**, 461 (2009).
[11] X.W. Liu, L. Lin, J.L. Lu, Y.D. Chen, D.S. Zhang. *J. Coord. Chem.*, **64**, 4344 (2011).
[12] D. Chatterjee, A. Sengupta, R. van Eldik. *J. Coord.Chem.*, **64**, 30 (2011).
[13] Y.J. Liu, C.H. Zeng, H.L. Huang, L.X. He, F. Eur. *J. Med. Chem.*, **45**, 564 (2010).
[14] L. Xu, N.J. Zhong, Y.Y. Xie, H.L. Huang, Z.H. Liang, Z.Z. Li, Y.J. Liu. *J. Coord. Chem.*, **65**, 55 (2012).
[15] H.J. Yu, Y. Chen, L. Yu, Z.F. Hao, L.H. Zhou. *Eur. J. Med. Chem.*, **55**, 146 (2012).
[16] K.J. Du, J.Q. Wang, J.F. Kou, G.Y. Li, L.L. Wang, H. Chao, L.N. Ji. *Eur. J. Med. Chem.*, **46**, 1056 (2011).
[17] A.R. Banerjee, J.A. Jaeger, D.H. Turner. *Biochemistry*, **32**, 153 (1993).
[18] A.E. Friedman, C.V. Kumar, N.J. Turro, J.K. Barton. *Nucleic Acids Res.*, **19**, 2595 (1991).
[19] J.C. Chambron, J.P. Sauvage, E. Amouyal, P. Koffi. *New J. Chem.*, **9**, 52 (1985).
[20] Y. Jenkins, A.E. Friedman, N.J. Turro, J.K. Barton. *Biochemistry*, **31**, 10809 (1992).
[21] A.E. Friedman, J.C. Chambron, J.P. Sauvage, N.J. Turro, J.K. Barton. *J. Am. Chem. Soc.*, **112**, 4960 (1990).
[22] Q.F. Guo, S.H. Liu, Q.H. Liu, H.H. Xu, J.H. Zhao, H.F. Wu, X.Y. Li, J.W. Wang. *J. Coord. Chem.*, **65**, 1781 (2012).
[23] U. Schatzschneider, J. Niesel, I. Ott, R. Gust, H. Alborzinia, S. Wölft. *ChemMedChem*, **3**, 1104 (2008).
[24] K. Wärnmark, J.A. Thomas, O. Heyke, J.M. Lehn. *Chem. Commun.*, **6**, 701 (1996).
[25] J.P. Collin, J.P. Sauvage. *Inorg. Chem.*, **25**, 135 (1986).
[26] R. Caspar, C. Cordier, J.B. Waern, C. Guyard-Duhayon, M. Gruselle, P.L. Floch, H. Amouri. *Inorg. Chem.*, **45**, 4071 (2006).
[27] A. Wolf, G.H. Shimer, Jr., T. Meehan. *Biochemistry*, **26**, 6392 (1987).
[28] C.C. Cheng, S.E. Rokita, C.J. Burrows. *Angew. Chem. Int. Ed. Engl.*, **32**, 277 (1993).
[29] T. Mosmann. *J. Immunol. Methods*, **65**, 55 (1983).
[30] K.K. Lo, T.K. Lee, J.S. Lau, W.L. Poon, S.H. Cheng. *Inorg. Chem.*, **47**, 200 (2008).
[31] D.L. Arockiasamy, S. Radhika, R. Parthasarathi, B.U. Nair. *Eur. J. Med. Chem.*, **44**, 2044 (2009).
[32] H.L. Huang, Z.Z. Li, Z.H. Liang, Y.J. Liu. *Eur. J. Inorg. Chem.*, **36**, 5538 (2011).
[33] R. Nilsson, P.B. Merkel, D.R. Kearns. *Photochem. Photobiol.*, **16**, 117 (1972).